

## Species assemblages of key prey taxa from the Southern Ocean and the Southern Indian Ocean using biogeographic networks

V. Djian<sup>1,2,3</sup>✉, C. Merland<sup>1,4</sup>, M. Thellier<sup>1,2</sup>, B. Leroy<sup>2</sup>, C. Cotte<sup>1</sup> and P. Koubbi<sup>1,3</sup>.

<sup>1</sup> LOCEAN-IPSL – Sorbonne Université, CNRS, IRD, MNHN, Laboratoire d’Océanographie et du Climat: Expérimentations et Approches Numériques, 4, place Jussieu, Boite 100 . F-75252 Paris Cedex 05  
France

<sup>2</sup> Laboratoire de Biologie des Organismes et Ecosystèmes Aquatiques (BOREA) MNHN, CNRS,IRD, SU, UCN, UA  
45 rue Buffon, 75231 Paris Cedex 05  
France

<sup>3</sup> IFREMER Centre Manche Mer du Nord. Unité Halieutique Manche Mer du Nord  
150 quai Gambetta, 62321 Boulogne-sur-Mer  
France

<sup>4</sup>: Institut de la Mer de Villefranche, IMEV Sorbonne Université-CNRS,  
181 Chemin du Lazaret, 06230 Villefranche-sur-Mer  
France

Email: [valentin.djian@sorbonne-universite.fr](mailto:valentin.djian@sorbonne-universite.fr)

### Abstract

Plankton plays an important role in the functioning of marine ecosystems, for example, through their role as prey. It is therefore important to understand the spatial distribution of assemblages of key taxa. This study aimed to determine the effect of hydrologic and topographic features on two major macrozooplankton groups: euphausiids and amphipods, which are important prey of seabirds and marine mammals. The biogeography of these taxa’s species between the Southern Indian Ocean and the North Indian sector of the Southern Ocean will be assessed by network analyses on species abundances. Our results from the REPCCOAI surveys from 2017 to 2019 between Crozet, Kerguelen and St Paul and New Amsterdam revealed a strong biogeographic separation between the subtropical and subantarctic zones. Species assemblages for each major taxon revealed a distinction between off shelf areas and the neritic zone and between high and low productivity areas, underlining the role of the subantarctic islands and their effect on primary production in the biogeography of the southern plankton. In the subtropical Indian Ocean, no significant major distinction was observed with the network analysis, even if some sites seem to show an influence of the Agulhas Return Current.

## Résumé

Le plancton joue un rôle important dans le fonctionnement des écosystèmes marins, notamment en tant que proie. Il est donc important de comprendre la distribution spatiale des assemblages de taxons clés. Cette étude visait à déterminer l'effet des caractéristiques hydrologiques et topographiques sur deux grands groupes de macrozooplancton : les euphausiacés amphipodes, qui constituent des proies importantes pour les oiseaux et les mammifères marins. La biogéographie des espèces de ces taxons entre le sud de l'océan Indien et le secteur nord de l'océan Indien dans l'océan Austral sera évaluée à l'aide d'analyses de réseau sur l'abondance des espèces. Nos résultats issus des campagnes REPCCOAI menées entre 2017 et 2019 entre Crozet, Kerguelen, Saint-Paul et Amsterdam ont révélé une forte séparation biogéographique entre les zones subtropicales et subantarctiques. Les assemblages d'espèces pour chaque taxon majeur ont révélé une distinction entre les zones au large des côtes et la zone néritique, ainsi qu'entre les zones à forte et faible productivité, soulignant le rôle des îles subantarctiques et leur effet sur la production primaire dans la biogéographie du plancton austral. Dans l'océan Indien subtropical, aucune distinction majeure n'a été observée à l'aide de l'analyse de réseau, même si certains sites semblent montrer une influence du courant de retour des Aiguilles.

## Абстракт

Планктон играет важную роль в функционировании морских экосистем, например, выступая в качестве корма для других организмов. Поэтому важно понимать пространственное распределение сообществ ключевых таксонов. Целью данного исследования было определить влияние гидрологических и топографических особенностей на две основные группы макрозоопланктона: эвфаузиды и амфиподы, которые являются важной добычей морских птиц и морских млекопитающих. Биogeография видов этих таксонов между южной частью Индийского океана и северо-восточным сектором Южного океана получит оценку на основе сетевого анализа по численности видов. Результаты съемок по программе REPCCOAI, проведенных с 2017 по 2019 год между островами Крозе, Кергелен, Сен-Поль и Новый Амстердам, выявили четкое биogeографическое разделение между субтропической и субантарктической зонами. Видовые сообщества по каждому основному таксону показали различное распределение между шельфовыми и прибрежными зонами, а также между районами с высокой и низкой продуктивностью, что подчеркивает роль субантарктических островов и их влияние на первичную продукцию в биogeографии южного планктона. В субтропической зоне Индийского океана при проведении анализа на основе сети не было обнаружено значительных различий, хотя в некоторых точках наблюдается влияние Обратного течения мыса Агульяс.

## Resumen:

El plancton desempeña un papel importante en el funcionamiento de los ecosistemas marinos, por ejemplo, como presa. Por esta razón, es importante conocer la distribución espacial de las agrupaciones de taxones clave. El objetivo de este estudio es determinar el efecto de las características hidrológicas y topográficas sobre dos grandes grupos de macrozooplancton: los euphausiidos y los anfipodos, que son presas importantes de aves y mamíferos marinos. Se evalúa la biogeografía de las especies de estos taxones en la confluencia entre el Océano Índico Meridional y el sector índico septentrional del Océano Austral mediante un análisis de redes de la abundancia de las especies. Nuestros resultados derivados de los estudios REPCCOAI (2017 a 2019) entre Crozet, Kerguelén y St Paul y Nueva Ámsterdam revelan una marcada separación biogeográfica entre las zonas subtropical y subantártica. Las agrupaciones de especies de cada taxón principal revelan una distinción entre zonas fuera de la plataforma y la zona nerítica y entre zonas de alta y baja productividad, lo que subraya el papel de las islas subantárticas y su efecto sobre la producción primaria en la biogeografía del plancton austral. En el Océano Índico subtropical, el análisis de redes no muestra diferencias significativas, aunque algunos sitios parecen presentar influencia de la corriente de retorno de Agulhas.

## Introduction

The Biogeographic Atlas of the Southern Ocean (De Broyer et al., 2014) synthesises knowledge of the Southern Ocean's biodiversity from historical explorations to the Census of Antarctic Marine Life (CAML) (2005–2010) which brought a tremendous amount of knowledge during the International Polar Year (2007–2009). CAML surveys did not focus on the Subantarctic Zone, but the results of the atlas showed the intensity of sampling efforts and gaps per major taxa. The results of the atlas for euphausiids (Cuzin-Roudy et al., 2014) and pelagic amphipods (Zeidler and De Broyer, 2014), the two taxa that we are studying showed that the area around the Kerguelen Islands was well sampled, but not the rest of the Indian Ocean and even less so the Crozet Islands. The biogeographic atlas described the latitudinal zonation of Southern Ocean fauna according to the major northern fronts (Antarctic, Subantarctic and Subtropical) separating pelagic assemblages between the Southern Ocean and the

Indian Ocean, as observed recently with a new study on mesozooplankton (Vereshchaka et al., 2021). However, in the oceanic areas of the Crozet and Kerguelen Islands, the latitudinal biogeographic pattern is unusual, due to the geographical narrowing of some of these fronts in the vicinity of the archipelagos (Figure 1). This situation is therefore of great interest for understanding the biogeographical role of each of the fronts and of the geomorphology. In this area, when studying fish larvae assemblages, Koubbi (1993) showed that the Subantarctic Front (SAF) was the major biogeographic barrier in this sector between the larvae of subtropical species and the Southern Ocean species. This was also supported by the biogeographic analysis of myctophids carried out by Koubbi et al. (2011). The present study therefore aims to test the importance of the different hydrologic zones and island shelves on the spatial distribution of macrozooplankton in the Indian subantarctic sector and the Southern Indian Ocean.

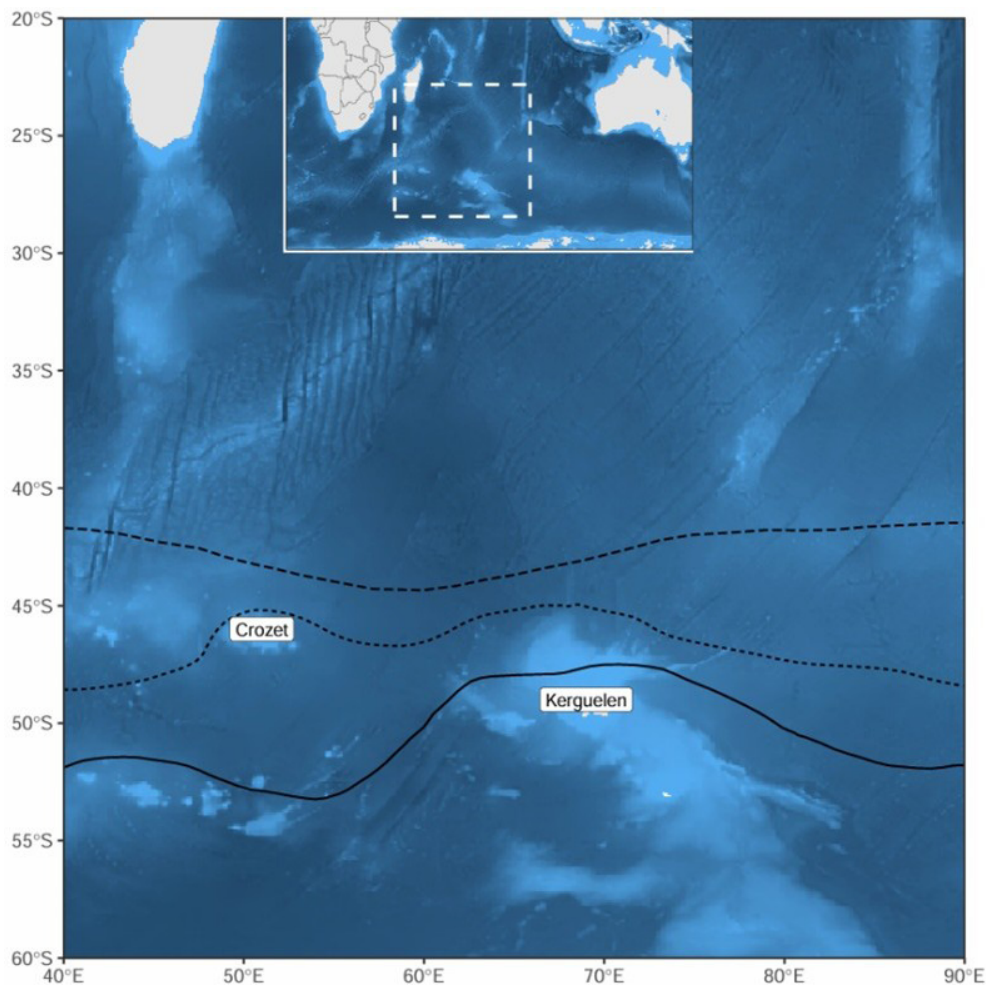


Figure 1: Map of the Indian sector of the subantarctic. The lines represent the fronts resulting from the ACC. The subtropical front is shown as a dashed line, the subantarctic front as a dotted line and the Antarctic polar front as a solid line.

## Material and methods

### Field sampling

The Response of the pelagic ecosystem to climate change in the Southern and South Indian Oceans (REPCCOAI) surveys were carried out each January–February in 2017, 2018 and 2019. During these surveys, macrozooplankton was sampled at each station with an Isaacs-Kidd Midwater Trawl net (IKMT). IKMT is a standard pelagic trawl net used for collecting macrozooplankton and micronekton. The net has a total length of 17 m, a metal wing, an opening area of 7 m<sup>2</sup> and a decreasing mesh size from 3.5 cm at the net entrance to 0.5 cm near the codend. The net was towed at a speed of between 2 and 3 knots. The IKMT was deployed obliquely from the surface to different water depths, mainly 200 m, 600 m or 1000–1200 m in order to sample both the epipelagic and the mesopelagic layers. The samples were preserved in a 5% buffered formalin solution. Macrozooplankton was sampled at a total of 82 stations in January and February 2017, 2018 and 2019 (Figure 1). The sampling network crossed oceanographic regions from the Indian subtropical zone to the Antarctic zone. The network covered a geographical area

between 50°E and 85°E and 27°S and 60°S and included the Crozet and Kerguelen archipelagos in the Southern Ocean and the islands of St. Paul and New Amsterdam in the Southern Indian Ocean. Some stations were also sampled on the shelves of Crozet, Kerguelen and Saint-Paul and New Amsterdam, but other coastal programs were more focused on this kind of study (Koubbi et al., 2009).

### Laboratory analysis

The samples were rinsed, then split using a Motoda box (Motoda, 1959), producing two equal fractions. For each taxonomic group (i.e. euphausiids and amphipods), counts were made in the fraction in which more than 100 individuals could be counted. Individuals were identified to species, when possible, using different taxonomic keys (Table 1). Count data were stored in a database and linked to the GPS coordinates of the sample, and converted to abundance (ind. 1000 m<sup>-3</sup>) using filtered seawater volume. The volume of filtered seawater was estimated (1) from the distance travelled by the net and its opening and (2) by flowmeters to calibrate calculations. Mapping of the main species' distribution of each taxonomic group is described by Merland et al. (2025).

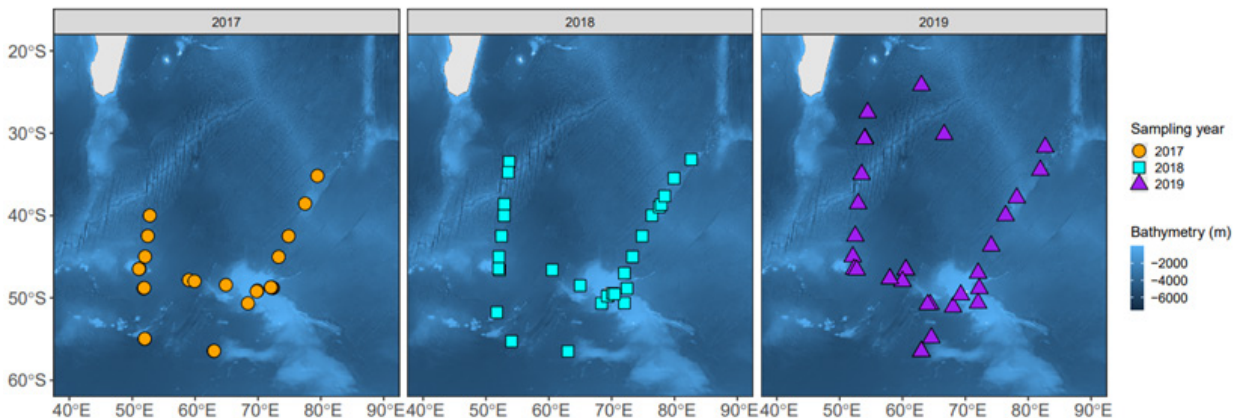


Figure 2: Map of sampling sites of the REPCCOAI surveys from 2017 to 2019.

Table 1: Taxonomic keys used for the identification of zooplankton taxonomic groups.

Taxonomic group	Taxonomic keys used
Euphausiids	Kirkwood, 1982; Boltovskoy, 1999.
Amphipods	Boltovskoy, 1999.

### Numerical analysis

We used biogeographic network analyses to identify species assemblages from abundance data independently for euphausiids and amphipods as we wanted to evaluate if the biogeographic boundaries were the same between these two groups. The ‘biogeonetworks’ R package by Leroy (version 0.1.2, 2019) was employed for this purpose. This approach, based on graph theory (Vilhena and Antonelli, 2015), involved creating a network with two types of nodes representing sampling sites and species found at those sites. Links were drawn between nodes when a species was identified at a particular site. The ‘Map Equation’ community-detection algorithm ([www.mapequation.org](http://www.mapequation.org), version 0.19.12, Rosvall and Bergstrom, 2008), known for its applicability in biogeographical studies (Vilhena and Antonelli, 2015; Leroy et al., 2019), was applied to the networks. This algorithm grouped nodes into clusters based on high intra-group and low inter-group connectivity, aligning with the concept of biogeographic regions. The algorithm was run with 1000 trials for each taxon to find optimal clustering. The resulting networks were visualised using the Gephi software (version 0.10, Bastian et al., 2009) with the ‘Force Atlas’ algorithm in order to group nodes that are strongly interconnected (i.e. assemblages that share species in common) and spread away from all other nodes that are not interconnected. The coloration of links

between nodes is the same as their source node, highlighting intergroup connections. For each taxonomic group, we grouped taxa if their taxonomic identifications were close together (i.e. genus species and genus cf. species) and excluded taxa that grouped several species due to uncertainty in identification. Starting with 49 amphipod taxa and 44 euphausiid taxa (Merland et al., 2025), we refined the dataset to 37 amphipod taxa and 32 euphausiid taxa by also excluding genus-level identifications (Supplementary table 1).

We mapped the spatial distribution of the sites associated with the different species assemblages in order to compare it to the mean and variation of hydrologic regions’ spatial distribution over 10 years defined by Djian et al. (2025). We identified seven hydrologic regions (Figure 2a), four of which are in the Southern Indian Ocean and three in the Southern Ocean. In this study, the boundaries of these regions were defined, showing the stability of certain fronts (Polar Front, Subtropical Front, and Subantarctic Front), particularly when constrained by topographic factors north of the Crozet and Kerguelen Island shelves. At the opposite, the boundaries of the observed regions are more diffuse in the open subtropical and tropical ocean zones (Figure 2b). Additional details on these hydrologic regions are available in Table 2.

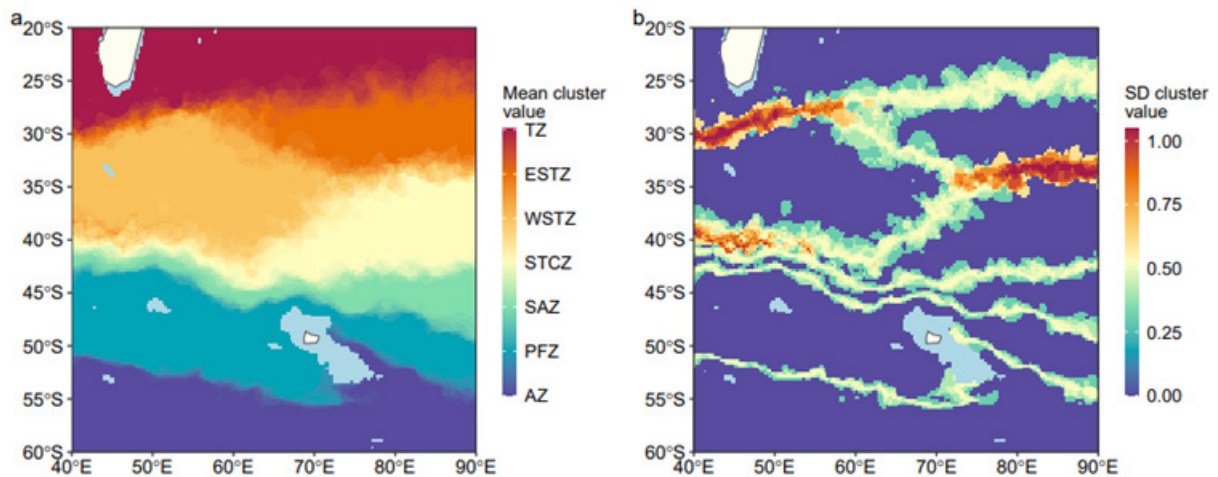


Figure 3: Mapping of a) mean and b) standard deviation of hydrologic cluster value for each cell between 2010 and 2020 identified by fPCA.

Table 2: Hydrologic regions and their characteristics defined by Djian et al. (2025).

Region number	Region's name	Code	Fronts/currents associated
1	Tropical Zone	TZ	South Equatorial Current
2	Eastern Subtropical zone	ESTZ	Indian Subtropical Gyre
3	Western Subtropical zone	WSTZ	East Madagascar Current
4	Subtropical Convergence Zone	STCZ	NSTF-SSTF
5	Subantarctic Zone	SAZ	SSTF-SAF
6	Polar Frontal Zone	PFZ	SAF-APF
7	Antarctic Zone	AZ	APF

We used the *IndVal* metric by Dufrêne and Legendre (1997) to determine indicator species for clusters identified at more than one site. The *IndVal* metric ranges from 0 to 1, with 0 indicating no presence of a species in a cluster and 1 indicating the presence of the species in all sites of the cluster. Indicator species for a cluster were identified as those with the maximum *IndVal* in that cluster. Abundance for the 15 most abundant species in each cluster seen on more than one site was represented, with boxplot transparency being proportional to their indicator value (i.e. indicator species will have their boxplot more opaque). To describe species assemblages in terms of diversity and abundance distribution, Hill numbers (Hill, 1973) were computed for each assemblage observed on more than one site using the ‘vegan’ R package (version 2.6, Oksanen et al., 2022). Hill numbers are a diversity measure that depends on a parameter  $q$ , and different values of  $q$  result in different diversity indices (Chao et al., 2014). For example, when  $q = 0$ , the Hill number simplifies to species richness, counting all species equally. For  $q = 1$ , the Hill number represents the effective number of abundant species, considering species in proportion to their abundances (i.e. Shannon Diversity). For  $q = 2$ , the Hill number corresponds to Simpson diversity, emphasising highly abundant species in the assemblage. These diversity measures help describe the total species richness, as well as the number of abundant and highly abundant species in the identified species assemblages.

## Results

### Euphausiid species assemblages

The Map Equation algorithm grouped REPCCOAI’s sampling sites into 6 distinct groups, with 3 being associated with distinct euphausiid species assemblages (Figure 4). Euphausiid group 1 (Figure 4, in pink) is defined only by *Euphausia vallentini*, this species being seen in the PFZ (Merland et al., 2025). Euphausiid group 2 (Figure 4, in purple) is defined by an assemblage of species found in the PFZ and the AZ, these species being *Thysanoessa macrura*, *Euphausia triacantha*, *Euphausia frigida* and *Euphausia superba*. Euphausiid group 3 (Figure 4, in green) identifies mainly tropical species, such as *Thysanopoda aequalis* et *Thysanopoda orientalis*, and subtropical species, such as *Euphausia spinifera*, *Euphausia similis* v. *armata* or *Stylocheiron maximum*, into another distinct assemblage. Euphausiid group 4 (Figure 4, in pale green) identifies *Euphausia similis* and *Euphausia longirostris*, two species mainly found in the subtropical and subantarctic (Merland et al., 2025). Euphausiid group 5 (Figure 4, in blue-green) only consists of one sampling site linked to *E. vallentini*, *E. triacantha* and *T. macrura*, and euphausiid group 6 (Figure 4, in dark blue) only has one species, *Euphausia tenera*. Looking at the network, we can see 34 links between euphausiid group 1 and euphausiid group 2 (Table 3). Most of these links are between *E. vallentini*

and euphausiid group 2's sampling sites, meaning that this species can be found outside of euphausiid group 1. On the other hand, 16 links can be seen between euphausiid group 3 and euphausiid group 2 and 11 links between euphausiid group 3 and euphausiid group 1, meaning that finding a species from euphausiid group 3 in a sampling site from euphausiid group 1 and 2 is uncommon, and

vice-versa. For the remaining 3 euphausiid groups, each unique sampling site shares several species with the previously described assemblages. Moreover, euphausiid group 6's unique sampling site is also the only site where *Euphausia tenera* is present. As such, they are difficult to classify objects for the Map Equation algorithm, resulting in the creation of these groups.

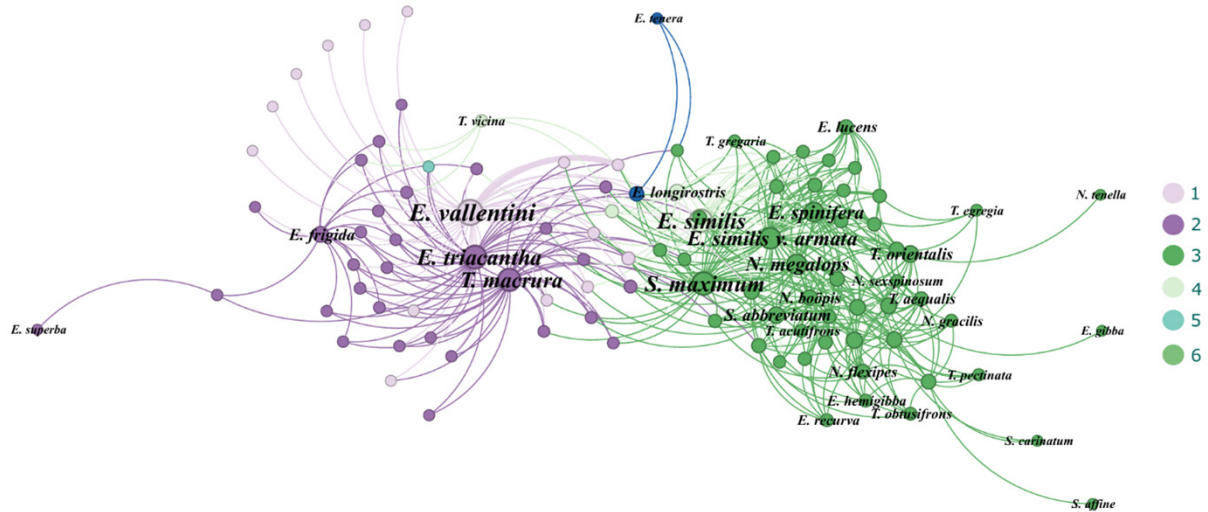


Figure 4: Biogeographic network of euphausiid raw abundance data. Colours indicate identified assemblages using the 'Map Equation' algorithm. Node size and node name size are proportional to their number of links.

Table 3: Diagonal matrix of the number of links between euphausiid assemblages. Number of intra-group links are shown in italic.

	1	2	3	4	5	6
1	<i>14</i>	34	11	6	1	1
2		<i>62</i>	16	11	2	2
3			<i>231</i>	35	0	5
4				<i>3</i>	0	3
5					<i>0</i>	0
6						<i>1</i>

Mapping of the sampling sites according to their euphausiid species group (Figure 5) allows us to distinguish spatial patterns in their distribution, mainly a separation at the Subantarctic Front (SAF). Euphausiid group 1 identifies sampling sites with high euphausiid abundance close to Crozet and Kerguelen islands (Figure 5, pink dots) in the PFZ (Figure 5, in light blue). It also identifies sites near the SAF between Crozet and Kerguelen. Euphausiid group 2 is also seen in the Southern Ocean, mainly in open ocean sampling sites (Figure 5, purple dots) from the PFZ and the AZ (Figure 5,

in blue). Euphausiid group 3 identifies all Indian Ocean sampling sites North of the SAF (Figure 5, green dots) the southern limit of the SAZ (Figure 5, in lime). For the last 3 euphausiid groups, they are only found at one sampling site each. Euphausiid group 4 (Figure 5, pale green dot) is seen at a sampling site close to the SAF, euphausiid group 5 (Figure 5, blue-green dot) is at a sampling site east of Kerguelen Island shelf and euphausiid group 6 (Figure 5, dark blue dot) is seen at a sampling site north of Crozet in the SAZ.

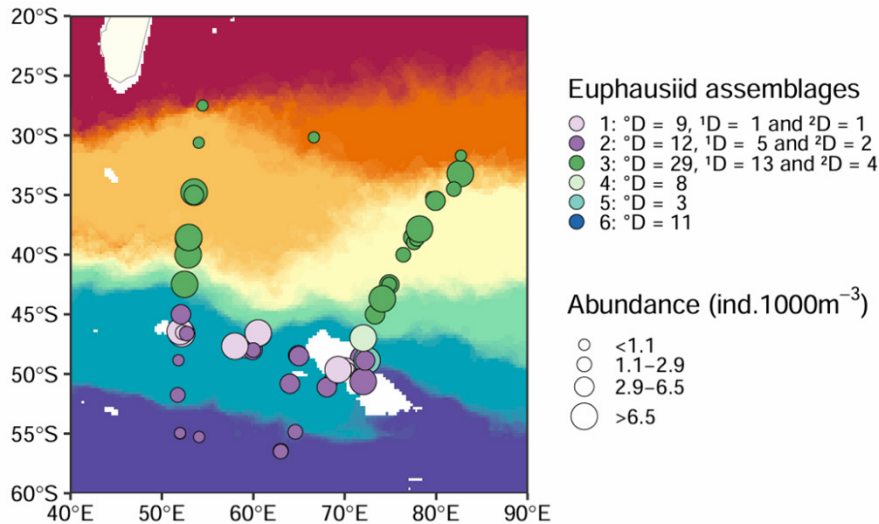


Figure 5: Spatial distribution of euphausiid species groups compared to mean distribution of the hydrologic regions identified by Djian et al. (2025). Colour represents the different species assemblages, and the size is proportional to quartile classes of total euphausiid abundance. For each assemblage, their respective Hill numbers are shown in the legend.

Looking at abundance and diversity, we can see that euphausiid assemblage 3 is by far the most diverse assemblage, having the highest species richness and the highest diversity. Its diversity is explained by the co-dominance of several subtropical species, the most abundant being *Euphausia spinifera* and *Nematoscelis megalops*, *E. similis* and *E. similis v. armata* (Figure 6, third panel). However, only *E. spinifera* and *E. similis v. armata* are indicative of this assemblage amidst these abundant euphausiid species (with indicator values being 0.82 and 0.61 respectively, see Table 4). On the other hand, some rare species, mostly tropical ones such as *Thysanopoda orientalis*, show high indicator values (of 0.60 for the latter). In contrast, euphausiid assemblage 1 has the lowest species richness and diversity of the study, which can be explained by the dominance of *E. vallentini* in euphausiid group 1's sampling sites where this

species shows its highest abundances, with 75% of the sites showing an abundance varying between 1.3 and 40.2 ind. 1000 m<sup>-3</sup> (Figure 6, first panel) and a maximum of more than 6000 ind.1000 m<sup>-3</sup>. This species defines euphausiid assemblage 1, as given by its indicator value of 0.99 for this assemblage (Table 4). Finally, euphausiid assemblage 2 shows higher species richness and diversity than euphausiid assemblage 1 (Figure 6, second panel). This higher diversity can be explained by the co-dominance of *E. triacantha*, one of the indicator species of euphausiid assemblage 2 (with an indicator value of 0.53) and *E. vallentini*, the indicator species of euphausiid assemblage 1. We can also see significant abundances of *E. frigida* and *T. macrura* in assemblage 2, who also have high indicator value for this assemblage (0.55 and 0.43 respectively).

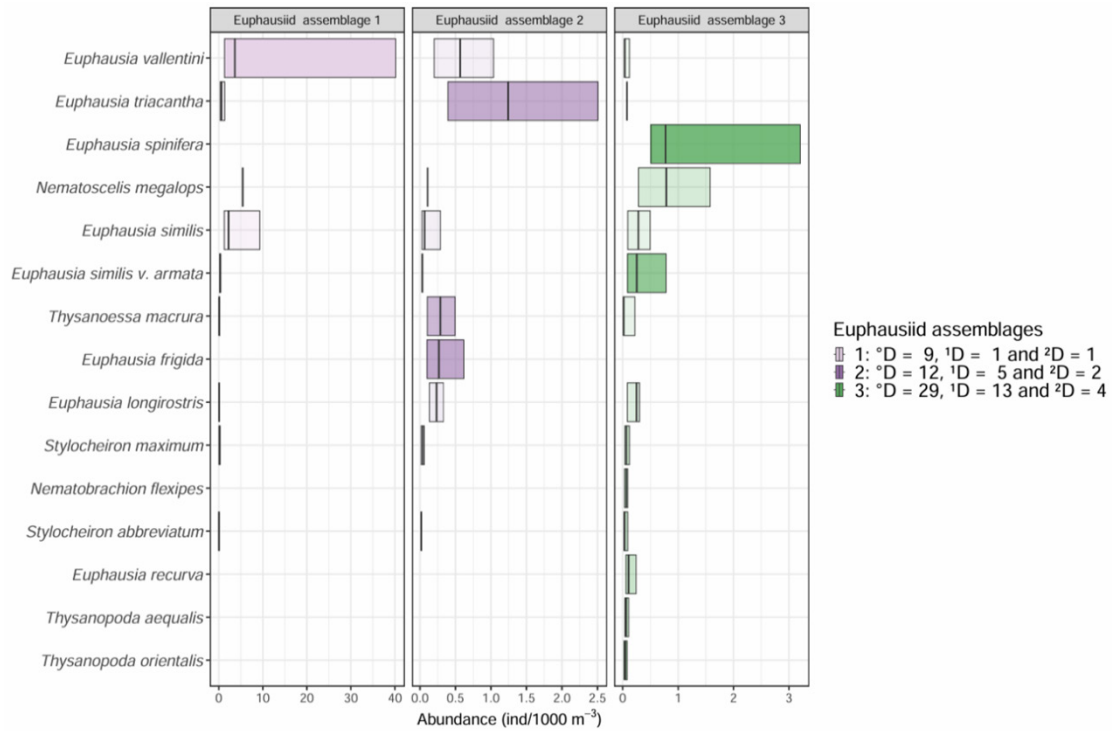


Figure 6: Bar plots of the abundance of the 15 most abundant euphausiid species in euphausiid species assemblages identified by the network analysis. Each bar plot is delimited by the first and third quartile, the black line being the median abundance of the species in the species assemblage. Opacity is proportional to the indicator value of the species for its assemblage. Only species assemblages with more than one sampling site are shown. For each assemblage, their respective Hill numbers are shown in legend.

Table 4: *IndVal* for Euphausiid assemblages.

Species assemblage	Lowest <i>IndVal</i>	Highest <i>IndVal</i>	Species with highest <i>IndVal</i>
1	0.016	0.998	<i>Euphausia vallentini</i>
2	0.001	0.556	<i>Euphausia frigida</i>
3	< 0.0001	0.821	<i>Euphausia spinifera</i>

Amphipod species assemblages

The Map Equation algorithm grouped REPCCOAI's sampling sites into 6 distinct amphipod groups (Figure 7). Amphipod group 1 (Figure 7, in purple) is defined by a species assemblage with *Themisto gaudichaudii*, a species found in most Antarctic and subantarctic sites and in some subtropical sites. This assemblage also has species only found in the PFZ and AZ such as *Cylopus magellanicus*, *Hyperoche medusarum*, *Lanceola clausii*, *Pegohyperia princeps* and *Orchomenella sp.* Amphipod group 2 (Figure 7, in pink) identifies several species found in the PFZ and AZ into another assemblage, including *Cyphocaris richardi*, *Cyphocaris challenger*, *Parandania boeckii* and *Lanceola serrata*. Amphipod group 3 (Figure 7, in green) identifies the species *Vibilia stebbingi*, *Vibilia viatrix*, *Phronima atlantica* and *Hyperia sp.*, which are only found in 2 sampling sites. Amphipod group 4 (Figure 7, in light blue) is defined by an assemblage with *Primno macropa*, a species found from the STCZ to the PFZ. It is followed by *Eurythenes obesus*, which is found

from the STCZ to the AZ, *Harleledo curvidactyla* and *Vibilia antarctica*, which are both found in the PFZ and AZ. Amphipod group 5 (Figure 7, in dark green) is defined by an assemblage of subtropical species, such as *Phronima sedentaria*, *Phrosina semilunata* or *Platyscelus ovoides*. Finally, amphipod group 6 (Figure 7, in light green) only has one species, *Paratyphis sp.* at one sampling site. When we look at the connectivity among the Southern Ocean groups, we can see that amphipod group 1 and amphipod group 2 are connected by 50 links between their respective nodes (Table 5). We can see similar numbers of links between group 1 and group 3, and between group 2 and group 3. This means that species of one assemblage can likely also be found at sampling sites of other assemblages. On the other hand, the number of links between these 3 Southern Ocean amphipod groups and group 5 is only half the number of links between the Southern Ocean groups. This means that it is less likely to have species related to amphipod assemblages 1, 2 and 4 in amphipod assemblage 5's sampling sites, and vice-versa.

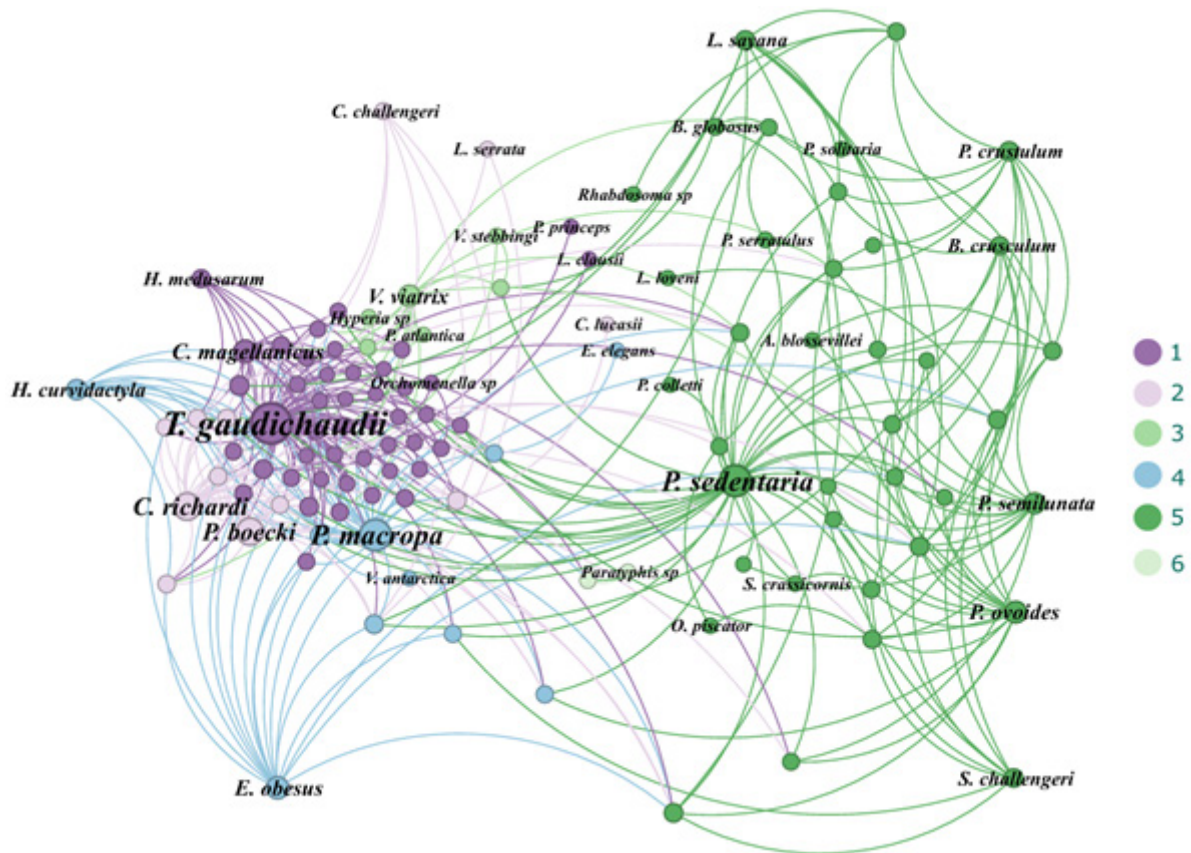


Figure 7: Biogeographic network of amphipod raw abundance data. Colours indicate identified assemblages using the ‘Map Equation’ algorithm. Node size and node name size are proportional to their number of links.

Table 5: Diagonal matrix of the number of links between euphausiid assemblages. Number of intra-assemblage links are shown in italic.

	1	2	3	4	5	6
1	<i>53</i>	62	31	69	34	19
2		<i>6</i>	21	50	29	17
3			<i>2</i>	19	12	3
4				<i>11</i>	33	17
5					<i>99</i>	4
6						<i>1</i>

Mapping of the sampling sites according to their amphipod species groups (Figure 7) allows us to see that a shift in assemblages is seen at the Southern Subtropical Front (SSTF), the northern boundary of the Subantarctic Zone (SAZ) (Figure 7, in lime). Amphipod group 1 (Figure 8, purple dots) mainly identifies sampling sites with high amphipod abundance close to Crozet and Kerguelen Islands in the PFZ (Figure 8, in light blue). On the other hand, amphipod group 2 (Figure 8, pink dots) identifies open ocean sampling sites from the PFZ in the inter-island area and the AZ (Figure 8, in blue).

Amphipod assemblage 3 (Figure 8, green dots) is seen at one site in the Western Subtropical Zone (WSTZ) (Figure 8, in orange) and another South of the SAF. Amphipod group 4 (Figure 8, light blue dots) is the last assemblage seen in the Southern Ocean, in sampling sites from and near the southern boundary of the SAZ (Figure 8, in lime). Out of the Southern Ocean, all sampling sites north of the SAF are grouped in the amphipod group 5 (Figure 8, dark green dots). Finally, amphipod group 6 (Figure 8, light green dot) is only found at a sampling site above Crozet in the SAZ.

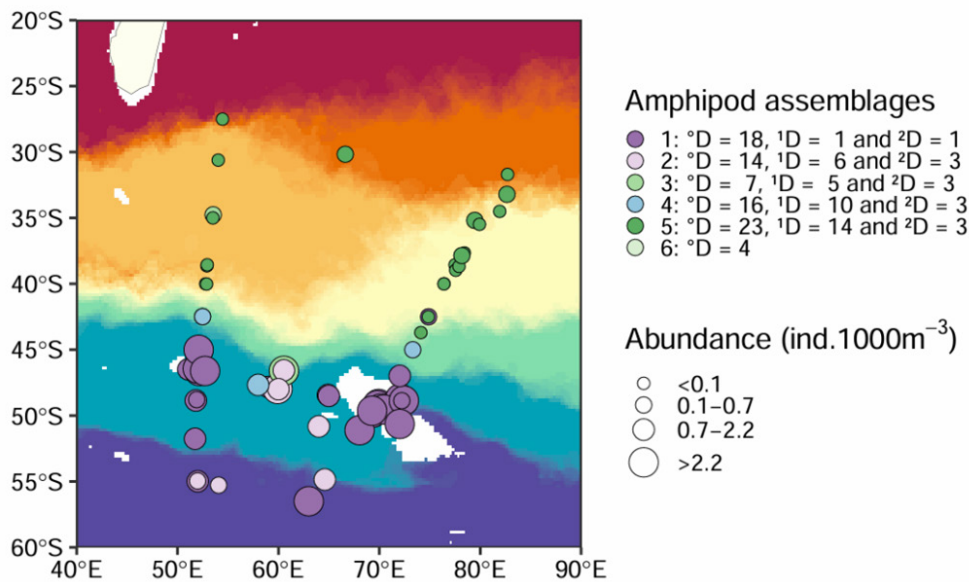


Figure 8: Spatial distribution of amphipod species groups compared to mean distribution of the hydrologic regions identified by Djian et al. (2025). Colour represents the different species assemblages, and the size is proportional to quartile classes of total amphipod abundance. For each assemblage, their respective Hill numbers are shown in legend.

Looking at abundance and diversity, we can see that all amphipod assemblages show similar diversity, except amphipod assemblage 1 (Figure 9, first panel). This can be explained by the complete dominance of *T. gaudichaudii* in amphipod assemblage 1's sampling sites. This species dwarves the other amphipod species found in this assemblage in terms of abundance, with 75% of the sites showing an abundance varying between 0.7 and 4.3 ind. 1000 m<sup>-3</sup> (Figure 9, first panel), with maximum observed abundance reaching 652 ind. 1000 m<sup>-3</sup>. It defines amphipod assemblage 1, being the only species with a high indicator value for this assemblage (Table 6). All remaining assemblages have similar diversity in terms of number of dominant species and differ in species richness and diversity. Amphipod assemblage 2 (Figure 9, second panel) shows a lower species richness than amphipod assemblage 1 but a higher overall diversity, which is explained by the increase in abundance of *P. boeckii*, the species with the highest indicator values of this assemblage (Table 6), and *C. richardi*, coupled with the decrease in abundance of *T. gaudichaudii* compared to amphipod assemblage 1. Amphipod assemblage 4 (Figure 9, fourth panel) has a similar species richness than amphipod assemblage 2 with a slightly higher species

diversity. Their species composition is also similar, but amphipod assemblage 4 distinguishes itself from amphipod assemblage 2 by high abundance of *P. macropa*, in similar values to *T. gaudichaudii*, the first being the species with the highest indicator value for amphipod assemblage 4 (Table 6). As for amphipod assemblage 5 (Figure 9, fifth panel), it shows the highest species richness and species diversity despite having a similar number of dominant species. This diversity can be explained by the co-abundance of several subtropical species, the most abundant being *P. sedentaria*, *P. semilunata* and *P. ovoides*, coupled with the presence of subantarctic species from the previous amphipod assemblages, such as *T. gaudichaudii*, *P. boeckii* or *P. macropa*. Despite *P. sedentaria* being the most abundant species, *Phrosina semilunata* shows the highest indicator values for this assemblage (Table 6), where *P. sedentaria* has an indicator value of only 0.24. Finally, amphipod assemblage 3 (Figure 9, third panel) is the one with the lowest species richness and diversity, which can be explained by the fact that it is seen on only 2 sampling sites. These sites show the highest abundance of *V. viatrix* (Figure 9, third panel) and *Hyperia* sp. and are the only sites where *P. atlantica* is observed.

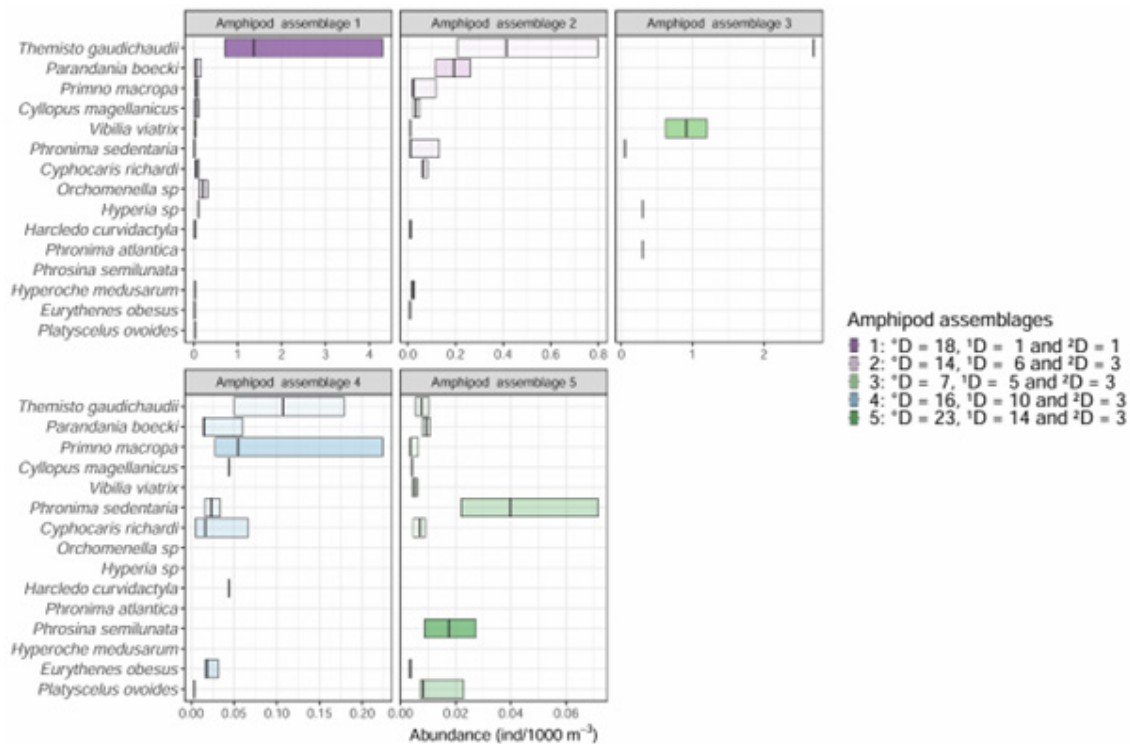


Figure 9: Barplots of the abundance of the 15 most abundant amphipod species in amphipod species assemblages identified by the network analysis. Each barplot is delimited by the first and third quartile, the black line being the median abundance of the species in the species assemblage. Opacity is proportional to the indicator value of the species for its assemblage. Only species assemblages with more than one sampling site are shown. For each assemblage, their respective Hill numbers are shown in legend.

Table 6: *IndVal* values for Amphipod assemblages.

Species assemblage	Lowest <i>IndVal</i>	Highest <i>IndVal</i>	Species with highest <i>IndVal</i>
1	0.006	0.879	<i>Themisto gaudichaudii</i>
2	0.001	0.643	<i>Parandania boeckii</i>
3	0.044	0.947	<i>Vibilia viatrix</i>
4	0.009	0.44	<i>Primno macropa</i>
5	< 0.0001	0.636	<i>Phrosina semilunata</i>

## Discussion

The biogeographic network analysis reveals that the Subantarctic Zone (SAZ) is a significant biogeographic transition zone for euphausiids and amphipods between the Indian Ocean and the Southern Ocean. This confirms observations described for myctophid (Koubbi, 2003; Koubbi et al., 2011) and for mesozooplankton (Vereshchaka et al., 2021), where marked changes in species assemblages occur on either side of the SAZ. However, there are slight differences of spatial distribution of assemblages between the two taxa. For euphausiids, the change occurs south of the SAZ at the SAF, while for amphipods, it happens north of the SAZ at the SSTF. The barrier seems more sharp for euphausiids, as hinted by the low number of links between the subtropical and the subantarctic assemblages with mainly subtropical species seen North of the SAF. The observation of subtropical species as far south as 47°S may result from either mesoscale eddies from the fronts advecting alien species into the region (Pakhomov and Froneman, 2000) or from the spatial variability of the SAF and APF (Boden and Parker, 1986). Conversely, the barrier seems less sharp for amphipods, as shown by the links between the subtropical and subantarctic assemblages, resulting from subantarctic species being seen as far north as 35°S in the eastern part of the STCZ. This absence of subantarctic species only in the western part of the study area could be related to the action of the ‘triple front’ to the north of Crozet which includes the SAF, the STF and the Agulhas Return Current Front (Belkin and Gordon, 1996).

## Biogeographic networks and species assemblages

The biogeographic network analysis on euphausiids and amphipods did not identify distinctions in the Southern Indian Ocean but highlighted distinction between neritic and open ocean sites in the PFZ. Neritic sites are associated with the highest total abundance of all sites for each taxon, due to high abundance of *E. vallentini* and *T. gaudichaudii* respectively. Both species have been found near island shelves with high abundance (Hunt and Pakhomov, 2003; Hunt and Swadling, 2021; Cotté et al., 2022), highlighting the strong productivity seen around the subantarctic islands due to natural iron fertilisation and island mass effects (Doty and Oguri, 1956; Blain et al., 2007). In the case of amphipods, this distinction can be explained by the more oceanic and mesopelagic distribution of *P. macropa* (Bocher et al., 2000) and *P. boeckii* (Hunt and Swadling, 2021) compared to *T. gaudichaudii*, which does not seem to undergo significant diel vertical migration and occurs in the epipelagic layer (Hunt and Swadling, 2021). Limited advection onto shallow shelf waters of mesopelagic plankton may also explain the limited abundance of both mesopelagic species in neritic sites (Hunt and Pakhomov, 2003). Moreover, the distinction in species assemblages between the subantarctic sites and the polar front and Antarctic sites by the relative abundance of *P. macropa* suggests that the latter may be an indicator species for the Subantarctic Zone, even though we didn’t find any studies addressing this subject. However, the distinction between neritic sites from the PFZ and open water sites observed in euphausiids’ species assemblages does not seem to be explained by differences in species spatial distribution. *E. triacantha* and *E. vallentini* are both

typical species of the PFZ on the opposite of *E. frigida*, which occurs in the AZ (Kirkwood, 1984; Cuzin-Roudy et al., 2014). Moreover, all three species occupy the same depth and seem to have the same patterns of diel vertical migration (Hunt and Swadling, 2021). The distinction in terms of species assemblages in the Southern Ocean cannot be explained like the amphipod species assemblages in the same area by the difference in bathymetry. We suggest that euphausiid assemblage 1 defined by *E. vallentini* reflects areas of high productivity, such as the subantarctic island shelves fertilised by iron which induces phytoplankton blooms (Doty and Oguri, 1956; Blain et al., 2007) and frontal zones (Lutjeharms et al., 1985; Strass et al., 2002), whereas the assemblage defined by *E. triacantha*, *T. macrura* and *E. frigida* is indicative of less productive open ocean zones. This opposition between these euphausiid assemblages may be explained by their dietary preference. The diet of *E. vallentini* has a high proportion of phytoplankton, indicating a tendency towards herbivory (Gurney et al., 2001; Mayzaud et al., 2003), whereas *E. triacantha* and *T. macrura* have a higher proportion of zooplankton in their diet, indicating a tendency towards omnivory or even carnivory (Phleger et al., 1998; Mayzaud et al., 2003). We can assume that in areas of high primary productivity, *E. vallentini* responds more quickly to the bloom by feeding directly on phytoplankton, allowing its populations to have blooms of high abundances, which allow them to dominate the euphausiid assemblage in these productive areas. Conversely, in areas of the open ocean where chlorophyll concentrations are lower, euphausiids with a carnivorous tendency are not solely dependent on phytoplankton, allowing them to maintain larger populations than *E. vallentini*.

## Conclusion

This study confirmed the strong influence of the latitudinal environmental gradient on the distribution of macrozooplankton species between the Southern Indian Ocean and the North Indian sector of the Southern Ocean, as well as the biogeographic importance of the Subantarctic Zone (SAZ), which forms a relatively strong barrier between the subtropical and subantarctic faunas in the study area. The approach based on the two major taxa, euphausiids and amphipods, analysed separately also allowed us to identify similar global

distribution patterns of assemblages with some local differences observed. This study showed that the biogeographic network method, coupled with the ‘Map Equation’ clustering algorithm, is suitable for visualising regions separated by ecotones. However, we have not observed subdivisions in the subtropical area in terms of species assemblages using this method, even though species distribution hinted at some differences between the western and the eastern part of the Indian sector of the Southern Ocean (Merland et al., 2025). We suppose that the differences between subtropical sites in terms of amphipods and euphausiid species distribution and abundance were not strong enough for the Map Equation algorithm to identify distinct species assemblages.

Macrozooplankton plays a key role in ecosystem functioning as a food source for top predators. The influence of the environment on their distribution is important in the context of global warming, which is particularly affecting the Southern Ocean (Frölicher et al., 2015; Meredith et al., 2019). According to Reygondeau et al. (2020), these changing environmental conditions would result in a southward shift of the epipelagic biogeochemical provinces of Longhurst (2007). This could lead to changes in the functioning of subantarctic ecosystems. It would be interesting to investigate the impact of global change on the distribution and biogeography of the species assemblages identified in this study.

## Acknowledgements

The samples analysed come from the REPCCOAI surveys directed by Philippe Koubbi and Jean-Yves Toullec (Roscoff Biological Station). It is part of the Zone Atelier Antarctique of CNRS. This article is a contribution to the Pelagic High seas eCoregionalisation of the Indian Subantarctic Zone (PHOCIS) project. We would like to thank ASOC for funding the Master’s degree internship that served as the basis of this article. We would also like to thank the *Office français de la biodiversité* (OFB) for their financial support on PHOCIS for the extension of high-sea marine protected areas (MPAs) within the CCAMLR area. This report is a contribution to the pelagic ecoregionalisation of the subantarctic (Makhado et al., 2019, 2023).

## References

- Adams, N.J. and N.T. Klages. 1989. Temporal Variation in the Diet of the Gentoo Penguin *Pygoscelis papua* at Sub-Antarctic Marion Island. *Col. Waterbirds*, 12(1): 30–36. <https://doi.org/10.2307/1521309>.
- Bastian, M., S. Heymann and M. Jacomy. 2009. Gephi: An Open Source Software for Exploring and Manipulating Networks. *Proceedings of the International AAAI Conference on Web and Social Media*, 3(1): 361–362. <https://doi.org/10.1609/icwsm.v3i1.13937>.
- Belkin, I.M. and A.L. Gordon. 1996. Southern Ocean fronts from the Greenwich meridian to Tasmania. *J. Geophys. Res. Oceans*, 101(C2): 3675–3696. <https://doi.org/10.1029/95JC02750>.
- Blain, S., B. Quéguiner, L. Armand, S. Belviso, B. Bomble, L. Bopp, A. Bowie, C. Brunet, C. Brussaard, F. Carlotti, U. Christaki, A. Corbière, I. Durand, F. Ebersbach, J.-L. Fuda, N. Garcia, L. Gerringa, B. Griffiths, C. Guigue, C. Guillerm, S. Jacquet, C. Jeandel, P. Laan, D. Lefèvre, C. Lo Monaco, A. Malits, J. Mosseri, I. Obernosterer, Y.-H. Park, M. Picheral, P. Pondaven, T. Remenyi, V. Sandroni, G. Sarthou, N. Savoye, L. Scouarnec, M. Souhaut, D. Thuiller, K. Timmermans, T. Trull, J. Uitz, P. van Beek, M. Veldhuis, D. Vincent, E. Viollier, L. Vong, and T. Wagener. 2007. Effect of natural iron fertilization on carbon sequestration in the Southern Ocean. *Nature*, 446: 1070–1074. <https://doi.org/10.1038/nature05700>.
- Bocher, P., Y. Cherel and K. Hobson. 2000. Complete trophic segregation between South Georgian and common diving petrels during breeding at Iles Kerguelen. *Mar. Ecol. Prog. Ser.*, 208: 249–264. <https://doi.org/10.3354/meps208249>.
- Boden, B.P. and L.D. Parker. 1986. The plankton of the Prince Edward Islands. *Polar Biol.*, 5: 81–93. <https://doi.org/10.1007/BF00443380>.
- Cushing, D.H. 1999. South Atlantic zooplankton. Boltovskoy, D. (Ed.). Backhuys, Leiden. *J. Plankton Res.*, 22(5): 997. <https://doi.org/10.1093/plankt/22.5.997>.
- Chao, A., N.J. Gotelli, T.C. Hsieh, E.L. Sander, K.H. Ma, R.K. Colwell and A.M. Ellison. 2014. Rarefaction and extrapolation with Hill numbers: a framework for sampling and estimation in species diversity studies. *Ecol. Monogr.*, 84(1): 45–67. <https://doi.org/10.1890/13-0133.1>.
- Cotté, C., A. Ariza, A. Berne, J. Habasque, A. Lebourges-Dhaussy, G. Roudaut, B. Espinasse, B.P.V. Hunt, E.A. Pakhomov, N. Henschke, C. Péron, A. Conchon, C. Koedooder, L. Izard and Y. Cherel. 2022. Macrozooplankton and micronekton diversity and associated carbon vertical patterns and fluxes under distinct productive conditions around the Kerguelen Islands. *J. Mar. Syst.*, 226: 103650. <https://doi.org/10.1016/j.jmarsys.2021.103650>.
- Cuzin-Roudy, J., J.O. Irisson, F. Penot, S. Kawaguchi and C. Vallet. 2014. Southern Ocean Euphausiids. In: De Broyer, C., P. Koubbi, H.J. Griffiths, B. Raymond, C. d’Udekem d’Acoz, A.P. Van de Putte, B. Danis, B. David, S. Grant, J. Gutt, C. Held, G. Hosie, F. Huettmann, A. Post and Y. Ropert-Coudert (Eds.). *Biogeographic Atlas of the Southern Ocean*. Scientific Committee on Antarctic Research, Cambridge: 309–320.
- De Broyer, C., P. Koubbi, H.J. Griffiths, B. Raymond, C. d’Udekem d’Acoz, A.P. Van de Putte, B. Danis, B. David, S. Grant, J. Gutt, C. Held, G. Hosie, F. Huettmann, A. Post and Y. Ropert-Coudert. (Eds.). 2014. *Biogeographic Atlas of the Southern Ocean*. Scientific Committee on Antarctic Research, Cambridge.
- Doty, M.S. and M. Oguri. 1956. The Island Mass Effect. *ICES J. Mar. Sci.*, 22(1): 33–37. <https://doi.org/10.1093/icesjms/22.1.33>.
- Djian, V., C. Cotté and P. Koubbi. 2025. Hydrologic regionalisation from Crozet to Kerguelen and subtropical Southern Indian Ocean. *CCAMLR Science*, 25: 1–18.
- Dufrêne, M. and P. Legendre. 1997. Species Assemblages and Indicator Species: the Need for a Flexible Asymmetrical Approach. *Ecol. Monogr.*, 67(3): 345–366. [https://doi.org/10.1890/0012-9615\(1997\)067\[0345:SAAI ST\]2.0.CO;2](https://doi.org/10.1890/0012-9615(1997)067[0345:SAAI ST]2.0.CO;2).

- Duhamel, G., P.-A. Hulley, R. Causse, P. Koubbi, M. Vacchi, P. Pruvost, S. Vignetta, J.-O. Irisson, S. Mormède, M. Belchier, A. Dettai, H. Williams, D.J. Gutt, C.D. Jones, K.-H. Kock, L.J. Lopez Abellan and A. Van de Putte. 2014. Biogeographic patterns of fish. In: De Broyer, C., P. Koubbi, H.J. Griffiths, B. Raymond, C. d'Udekem d'Acoz, A.P. Van de Putte, B. Danis, B. David, S. Grant, J. Gutt, C. Held, G. Hosie, F. Huettmann, A. Post and Y. Ropert-Coudert (Eds.). *Biogeographic Atlas of the Southern Ocean*. Scientific Committee on Antarctic Research, Cambridge: 328–362.
- Frölicher, T.L., J.L. Sarmiento, D.J. Paynter, J.P. Dunne, J.P. Krasting and M. Winton. 2015. Dominance of the Southern Ocean in Anthropogenic Carbon and Heat Uptake in CMIP5 Models. *J. Climate*, 28: 862–886. <https://doi.org/10.1175/JCLI-D-14-00117.1>.
- Gurney, L.J., P.W. Froneman, E.A. Pakhomov and C.D. McQuaid. 2001. Trophic positions of three euphausiid species from the Prince Edward Islands (Southern Ocean): implications for the pelagic food web structure. *Mar. Ecol. Prog. Ser.*, 217: 167–174.
- Hill, M.O. 1973. Diversity and Evenness: A Unifying Notation and Its Consequences. *Ecology*, 54(2): 427–432. <https://doi.org/10.2307/1934352>.
- Hunt, B.P.V. and E.A. Pakhomov. 2003. Mesozooplankton interactions with the shelf around the sub-Antarctic Prince Edward Islands archipelago. *J. Plankton Res.*, 25(8): 885–904. <https://doi.org/10.1093/plankt/25.8.885>.
- Hunt, B.P.V. and K.M. Swadling. 2021. Macrozooplankton and micronekton community structure and diel vertical migration in the Heard Island Region, Central Kerguelen Plateau. *J. Mar. Syst.*, 221: 103575. <https://doi.org/10.1016/j.jmarsys.2021.103575>.
- Kirkwood, J. M. 1982. A Guide to the Euphausiacea of the Southern Ocean, Vol. 1, *ANARE Res. Notes*. Information Services Section, Antarctic Division, Dept. of Science and Technology.
- Koubbi, P. 1993. Influence of the Frontal Zones on Ichthyoplankton and Mesopelagic Fish Assemblages in the Crozet Basin (Indian Sector of the Southern Ocean). *Polar Biol.*, 13: 557–564.
- Koubbi, P., M. Moteki, G. Duhamel, A. Goarant, P.-A. Hulley, R. O'Driscoll, T. Ishimaru, P. Pruvost, E. Tavernier and G. Hosie. 2011. Ecoregionalization of myctophid fish in the Indian sector of the Southern Ocean: Results from generalized dissimilarity models. *Deep-Sea Res. II: Top. Stud. Oceanog.*, 58(1–2): 170–180. <https://doi.org/10.1016/j.dsr2.2010.09.007>.
- Leroy, B. 2019. biogeonetworks: Biogeographical Network Manipulation And Analysis, R package version 0.1.2, <https://github.com/Farewe/biogeonetworks>.
- Leroy, B., M.S. Dias, E. Giraud, B. Hugué, C. Jézéquel, F. Leprieur, T. Oberdorff and P.A. Tedesco. 2019. Global biogeographical regions of freshwater fish species. *J. Biogeogr.*, 46(11): 2407–2419. <https://doi.org/10.1111/jbi.13674>.
- Longhurst, A.R. 2010. *Ecological Geography of the Sea*. Elsevier: 560 pp.
- Lutjeharms, J.R.E., N.M. Walters and B.R. Allanson. 1985. Oceanic Frontal Systems and Biological Enhancement. In: Siegfried, W.R., P.R. Condy and R.M. Laws (Eds.), *Antarctic Nutrient Cycles and Food Webs*. Springer, Berlin, Heidelberg: pp. 11–21. [https://doi.org/10.1007/978-3-642-82275-9\\_3](https://doi.org/10.1007/978-3-642-82275-9_3).
- Makhado, A.B., A. Lowther, P. Koubbi, I. Ansoorge, C. Brooks, C. Cotté, R. Crawford, S. Dzulisa, F. d'Ovidio, S. Fawcett, D. Freeman, S. Grant, J. Huggett, M. Hindell, P.A. Hulley, S. Kirkman, T. Lamont, M. Lombard, M.J. Masothla, M.-A. Lea, W.C. Oosthuizen, F. Orgeret, R. Reisinger, T. Samaai, S. Sergi, K. Swadling, S. Somhlaba, A. Van de Putte, C. Von de Meden and D. Yemane. 2019. Expert Workshop on Pelagic Spatial Planning for the eastern subantarctic region (Domains 4, 5 and 6). Document *SC-CAMLR-38/BG/29*. CCAMLR, Hobart, Australia, 71 pp.
- Makhado, A., P. Koubbi, J.A. Huggett, C. Cotté, R. Reisinger, K.M. Swadling, C. Azarian, C. Barnerias, F. d'Ovidio, L. Gauthier, E. Goberville, B. Leroy, A.T. Lombard, L. Muller, A. Van de Putte and workshop participants.

2023. Ecoregionalisation of the pelagic zone in the Subantarctic and Subtropical Indian Ocean. Document *SC-CAMLR-42/08*. CCAMLR, Hobart, Australia, 32 pp.
- Mayzaud, P., M. Boutoute and F. Alonzo. 2003. Lipid composition of the euphausiids *Euphausia vallentini* and *Thysanoessa macrura* during summer in the Southern Indian Ocean. *Antarct. Sci.*, 15(4): 463–475. <https://doi.org/10.1017/S0954102003001573>.
- Meredith, M., M. Sommerkorn, S. Cassotta, C. Derksen, A. Ekaykin, A. Hollowed, G. Kofinas, A. Mackintosh, J. Melbourne-Thomas, M.M.C. Muelbert, G. Ottersen, H. Pritchard, and E.A.G. Schuur. 2019. Polar Regions. In: Pörtner, H.-O., D.C. Roberts, V. Masson Delmotte, P. Zhai, M. Tignor, E. Poloczanska, K. Mintenbeck, A. Alegría, M. Nicolai, A. Okem, J. Petzold, B. Rama and N.M. Weyer (Eds.). *IPCC Special Report on the Ocean and Cryosphere in a Changing Climate*. Cambridge University Press, Cambridge, UK and New York, NY, USA: pp. 203–320. <https://doi.org/10.1017/9781009157964.005>.
- Merland, C., M. Thellier, V. Djian, C. Cotté and P. Koubbi. 2025. Macrozooplankton from Crozet to Kerguelen and subtropical Southern Indian Ocean. *CCAMLR Science*, 25: 99–116.
- Motoda, S. 1959. Devices of simple plankton apparatus. *Mem. Fac. Fish., Hokkaido Univ.*, 7(1-2): 73–94.
- Oksanen, J., G. Simpson, F. Blanchet, R. Kindt, P. Legendre, P. Minchin, R. O'Hara, P. Solymos, M. Stevens, E. Szoecs, H. Wagner, M. Barbour, M. Bedward, B. Bolker, D. Borcard, G. Carvalho, M. Chirico, M. De Caceres, S. Durand, H. Evangelista, R. FitzJohn, M. Friendly, B. Furneaux, G. Hannigan, M. Hill, L. Lahti, D. McGlinn, M. Ouellette, E. Ribeiro Cunha, T. Smith, A. Stier, C. Ter Braak and J. Weedon. 2022. *vegan: Community Ecology Package*. R package version 2.6-4, <https://CRAN.R-project.org/package=vegan>.
- Pakhomov, E.A. and P.W. Froneman. 2000. Composition and spatial variability of macroplankton and micronekton within the Antarctic Polar Frontal Zone of the Indian Ocean during austral autumn 1997. *Polar Biol.*, 23: 410–419. <https://doi.org/10.1007/s003000050462>.
- Reygondeau, G., W.W.L. Cheung, C.C.C. Wabnitz, V.W.Y. Lam, T. Frölicher and O. Maury. 2020. Climate Change-Induced Emergence of Novel Biogeochemical Provinces. *Front. Mar. Sci.*, 7: 657. <https://doi.org/10.3389/fmars.2020.00657>.
- Rosvall, M. and C.T. Bergstrom. 2008. Maps of random walks on complex networks reveal community structure. *Proc. Natl. Acad. Sci. U.S.A.*, 105(4): 1118–1123. <https://doi.org/10.1073/pnas.0706851105>.
- Strass, V.H., A.C. Naveira Garabato, R.T. Pollard, H.I. Fischer, I. Hense, J.T. Allen, J.F. Read, H. Leach and V. Smetacek. 2002. Mesoscale frontal dynamics: shaping the environment of primary production in the Antarctic Circumpolar Current. *Deep-Sea Res. II: Top. Stud. Oceanog.*, 49(18): 3735–3769. [https://doi.org/10.1016/S0967-0645\(02\)00109-1](https://doi.org/10.1016/S0967-0645(02)00109-1).
- Vereshchaka, A., E. Musaeva and A. Lunina. 2021. Biogeography of the Southern Ocean: environmental factors driving mesoplankton distribution South of Africa. *PeerJ*, 9: e11411. <https://doi.org/10.7717/peerj.11411>.
- Vilhena, D.A. and A. Antonelli. 2015. A network approach for identifying and delimiting biogeographical regions. *Nat Commun*, 6 : 6848. <https://doi.org/10.1038/ncomms7848>.
- Zeidler, W. and C. De Broyer. 2014. Amphipoda: Hyperiididae. In: De Broyer, C., P. Koubbi, H.J. Griffiths, B. Raymond, C. d'Udekem d'Acoz, A.P. Van de Putte, B. Danis, B. David, S. Grant, J. Gutt, C. Held, G. Hosie, F. Huettmann, A. Post and Y. Ropert-Coudert (Eds.). *Biogeographic Atlas of the Southern Ocean*. Scientific Committee on Antarctic Research, Cambridge: 309–320.

Table A1: Taxa retained for biogeographic network analysis.

<b>Taxonomic order</b>	<b>Taxa name</b>
Amphipoda	<i>Anchylomera blossevillei</i>
Amphipoda	<i>Bathystegocephalus globosus</i>
Amphipoda	<i>Brachyscelus crusculum</i>
Amphipoda	<i>Cyllopus lucasii</i>
Amphipoda	<i>Cyphocaris challengerii</i>
Amphipoda	<i>Cyphocaris richardi</i>
Amphipoda	<i>Eurythenes obesus</i>
Amphipoda	<i>Eusirella elegans</i>
Amphipoda	<i>Harledeo curvidactyla</i>
Amphipoda	<i>Hyperia sp</i>
Amphipoda	<i>Hyperoche medusarum</i>
Amphipoda	<i>Lanceola clausii</i>
Amphipoda	<i>Lanceola loveni</i>
Amphipoda	<i>Lanceola sayana</i>
Amphipoda	<i>Lanceola serrata</i>
Amphipoda	<i>Orchomenella sp</i>
Amphipoda	<i>Oxycephalus piscator</i>
Amphipoda	<i>Parandania boeckii</i>
Amphipoda	<i>Parapronoe crustulum</i>
Amphipoda	<i>Paratyphis sp</i>
Amphipoda	<i>Pegohyperia princeps</i>
Amphipoda	<i>Phronima atlantica</i>
Amphipoda	<i>Phronima colletti</i>
Amphipoda	<i>Phronima sedentaria</i>
Amphipoda	<i>Phronima solitaria</i>
Amphipoda	<i>Phrosina semilunata</i>
Amphipoda	<i>Platyscelus ovoides</i>
Amphipoda	<i>Platyscelus serratulus</i>
Amphipoda	<i>Primno macropa</i>
Amphipoda	<i>Rhabdosoma sp</i>
Amphipoda	<i>Scina crassicornis</i>
Amphipoda	<i>Streetsia challengerii</i>
Amphipoda	<i>Themisto gaudichaudii</i>
Amphipoda	<i>Vibilia antarctica</i>

Amphipoda	<i>Vibilia stebbingi</i>
Euphausiacea	<i>Euphausia gibba</i>
Euphausiacea	<i>Euphausia hemigibba</i>
Euphausiacea	<i>Euphausia longirostris</i>
Euphausiacea	<i>Euphausia lucens</i>
Euphausiacea	<i>Euphausia recurva</i>
Euphausiacea	<i>Euphausia similis</i>
Euphausiacea	<i>Euphausia similis v. armata</i>
Euphausiacea	<i>Euphausia spinifera</i>
Euphausiacea	<i>Euphausia superba</i>
Euphausiacea	<i>Euphausia tenera</i>
Euphausiacea	<i>Euphausia triacantha</i>
Euphausiacea	<i>Euphausia vallentini</i>
Euphausiacea	<i>Nematobranchion boöpis</i>
Euphausiacea	<i>Nematobranchion flexipes</i>
Euphausiacea	<i>Nematobranchion sexspinosum</i>
Euphausiacea	<i>Nematoscelis gracilis</i>
Euphausiacea	<i>Nematoscelis megalops</i>
Euphausiacea	<i>Nematoscelis tenella</i>
Euphausiacea	<i>Stylocheiron abbreviatum</i>
Euphausiacea	<i>Stylocheiron affine</i>
Euphausiacea	<i>Stylocheiron carinatum</i>
Euphausiacea	<i>Stylocheiron maximum</i>
Euphausiacea	<i>Thysanoessa gregaria</i>
Euphausiacea	<i>Thysanoessa macrura</i>
Euphausiacea	<i>Thysanoessa vicina</i>
Euphausiacea	<i>Thysanopoda acutifrons</i>
Euphausiacea	<i>Thysanopoda aequalis</i>
Euphausiacea	<i>Thysanopoda egregia</i>
Euphausiacea	<i>Thysanopoda obtusifrons</i>
Euphausiacea	<i>Thysanopoda orientalis</i>
Euphausiacea	<i>Thysanopoda pectinata</i>

